

# Mechanism and optimum pressure for sliding-mode nanogenerator

Hang Yun, Ren He

*School of Automotive and Traffic Engineering, Jiangsu University, Zhenjiang, 212013, China*

*\*Corresponding author: e-mail: 18352860963@163.com*

Triboelectric nanogenerator has extensive applicability because of its capability of harvesting mechanical energy and flexible working modes. To research the optimum pressure and improve the recovered energy of the sliding-mode triboelectric nanogenerator, a contact model of the Al/PTFE tribo-pair is studied by ab initio calculation and finite element simulation. The F-atom of PTFE is proved to be the electron acceptor and the charges transferred can be predicted by Bader charge analysis. The mathematical relation between interfacial distance, charges transferred and contact pressure can be fitted. By Gauss's law, the electric field is simulated and the regeneration energy of the sliding-mode triboelectric nanogenerator can be evaluated by the total electric energy and friction loss. Finally, an optimum pressure can be set to the upper or lower limit of working pressure corresponding to larger recovered energy. And less friction coefficient and larger contact area are also effective methods for recovering energy.

**Keywords:** triboelectric nanogenerator, ab initio calculation, optimum pressure, recovered energy.

## INTRODUCTION

This Triboelectric nanogenerator (TENG) plays an increasingly excellent role in energy recovery and self-powered sensing systems<sup>1,2</sup>. The mechanism is comprised of contact electrification (CE) for tribo-layers and electrostatic induction for electrodes. Ab initio calculation can be used to reflect the decrease of energy barrier and electron transition after the electron-clouds overlap<sup>3</sup>. On the other hand, by utilizing electrostatic induction which can be precisely described by Maxwell's theory of electromagnetism, electric potential energy can be effectively converted into electric energy<sup>4</sup>. The researches of the above two theories constantly improve the mechanism of TENG.

Ab initio calculation is based on density functional theory (DFT) and has developed rapidly with the advance of computer technology. By using programs for ab initio calculation, the electronic structures of two tribo-layers models and their CE results can be predicted and supported by experiments<sup>5,6</sup>. Wu et al. found that the lowest unoccupied molecular orbitals (LUMOs) of polyethylene terephthalate (PET) and polyimide (Kapton) were the electron acceptor when they contacted Al and the major electron-accept regions were carboxyl in PET and the imide in Kapton<sup>7</sup>. For the chemically identical tribo-pair with different surface curvatures, it can be predicted that flexoelectricity caused charge transfer by analyzing piezoelectric molybdenum telluride (2H-MoTe<sub>2</sub>) and non-piezoelectric graphene<sup>8</sup>. Moreover, it can be found by ab initio calculations that the surface defect could generate a trap state attracting a negative charge and humidity can promote contact charging<sup>9,10</sup>. Some researchers combined ab initio calculation and molecular dynamics (MD) simulation and revealed that the driving force of CE process probably originated from the potential gradient, not the work function<sup>11,12</sup>. According to the above ab initio calculations, the overlap of electron orbitals leads to a lower contact barrier and stronger electric field strength. Therefore, the CE phenomenon is common and easy to happen in the thin barrier of two tribo-layers. After CE occurs, the surface charge density can be considered as a constant on the polymer surface and the exponential decay of surface charge can be ignored in a small time scale<sup>13</sup>.

Another mechanism of TENG is electrostatic induction. Many researchers tended to assign surface charge densities of tribo-layers via experimental data and focus on the mathematical models of TENG in various working modes<sup>14</sup>. Wang's research team took the lead in studying the charging process of TENG with inherent capacitive behavior and deduced the equations of the amount of charge transferred and output voltage<sup>4</sup>. FEM calculations can help researchers build an accurate electric field for TENGs with various structures and motion speeds based on Maxwell's equations<sup>15</sup>. The parameters of TENG need to be optimized consisting of load resistance, permittivity, geometric configuration, mass<sup>16-19</sup>. It is necessary to optimize the TENG design to improve output performance.

Ab initio calculations for tribo-layer material modification and FEM calculations for TENG optimization have promoted the development of TENG. However, few studies combine the CE process and electrostatic induction to optimize some important physical quantities. Actually, there exist some physical variables that affect CE process and output performance of TENG.

In this paper, an Al/polytetrafluoroethylene (PTFE) contact model is studied by the mean of ab initio calculation. Every electronic structure of molecules is calculated under different external forces. The details of charge transferred are discussed by the density of states and Bader charge analysis. Then the relation between the amount of charge transferred and the contact pressure is fitted and applied to the FEM model which is used to simulate the electric field of sliding-mode TENG. Finally, the recovered energy is related to the contact pressure and friction loss, and the optimum pressure corresponding to the maximum recovered energy changes with the working pressure range and CE properties of tribo-layer materials.

## METHODE FOR AB INITIO CALCULATIONS

### Model and Parameters

The common Al/PTFE tribo-pair is used to be studied by Quantum-Espresso software package, which is based on density-functional theory, pseudopotentials and plane waves<sup>20</sup>. Perdew-Burke-Ernzerhof (PBE) functional is

utilized to describe the wavefunction, electron density and electric potential<sup>21</sup>.

Solid PTFE is a negative friction material for TENGs because it has a high capability of attracting and storing negative charges. PTFE has four phases and we adopt the molecular configuration of phase IV at room temperature and low pressure<sup>22</sup>.

Over 19 °C, the disorder of helical PTFE is caused by torsional oscillations coupled with a gradual untwisting and the internal rotational angle of the one-atom chain is 163.7°<sup>23</sup>. Considering the common preparation process of PTFE<sup>24</sup>, the configuration of PTFE parallel to another tribo-layer is wear-resistant and easy to process. Therefore, we adopt a helical PTFE chain with five C-atoms to contact the Al (1 1 1) surface. The relaxed structures of the PTFE chain and the Al (1 1 1) surface are combined into a CE model. Figure 1 is the initial configuration of the interfacial model and the external force is applied to the PTFE chain. The z-axis positions of underlying Al-atoms are fixed. A kinetic energy cutoff for wavefunctions is 50 Ry and a kinetic energy cutoff for charge density and potential is 500 Ry. The type of van der Waals correction is set to grimme-d3 which introduces longer range forces to the system and the thickness of vacuum layer is 18 Å. The boundary condition of the isolated system is set to bc3. A  $3 \times 3 \times 1$  k-point is utilized to take sample in the Brillouin zone. The contact pressure ranges from 0 to 500 MPa which can be converted into the current lattice's external forces.

## FIGURES

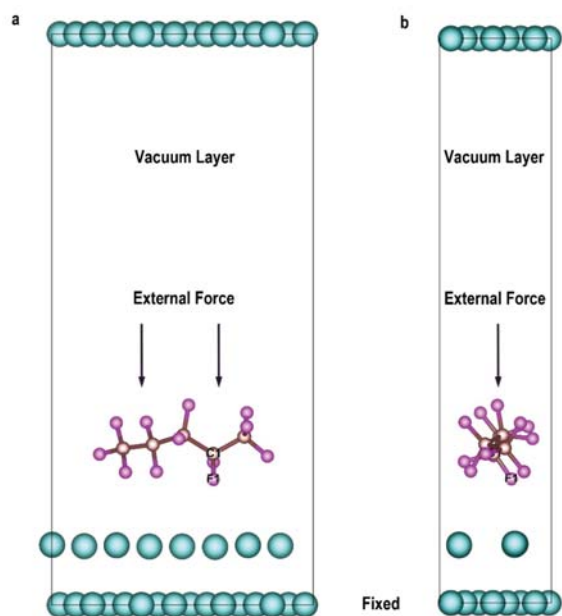


**Figure 1.** The initial configuration of the interfacial model

## RESULTS AND DISCUSSION

The PTFE chain approaches Al (1 1 1) surface under the external force and the center of mass of the system and every atom will move to the equilibrium position when the calculation converges. Bader charge analysis is a convenient tool and is adopted to calculate the charge of every atom. Figure 2 is the amounts of extra electrons attracted by F-atoms and Al-atoms under 500 MPa. A negative value means that the atom loses electrons and the abscissa represents the atomic number.

The number of extra electrons equal to the occupation of Bader charge minus the amount of valence charge of the certain atom. Figure 2 shows that every F-atom obtains about 0.9 electrons and every upper Al-atom loses about 0.65 electrons. Therefore, the Al-atoms in the surface layer participate in the CE process and F atoms are the electron acceptor in this system.

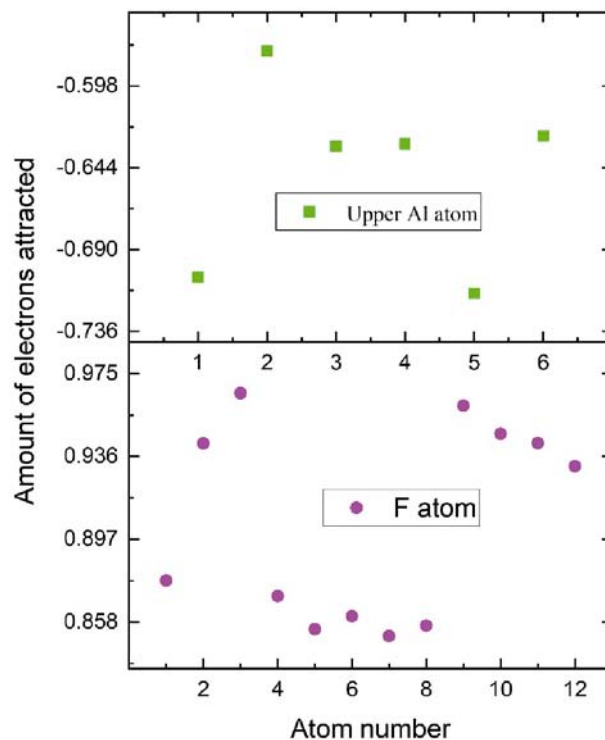


**Figure 2.** The amounts of extra electrons attracted under 500 MPa

To intuitively show the influence of external force on the electronic structures, we calculate the projected DOS of the 2p orbital of F-atom 1 and C-atom 1 under the contact pressure of 300 and 500 MPa which is shown in Figure 3. The above F-atom 1 and C-atom 1 are marked in Figure 1. Compared with the density of states under different contact pressures, the electrons of C and F atoms tend to appear in higher energy orbitals when the tribo-layers are under larger contact pressure. And the increase in the specific surface area of tribo-layers means that F-atoms are more exposed near the Al-atoms which will stimulate more CE sites.

Finally, the calculation results of the interfacial model with six contact pressures, namely 0, 100, 200, 300, 400, and 500 MPa, are processed and analysed as follows. Figure 4 shows the relationship between interfacial distance, charge transferred, and contact pressure. It is obvious that the interfacial distance is a monotonous decrease function of contact pressure and the constant slope of the relationship shows that Al and PTFE can be regarded as linear elastic materials below 500 MPa. Moreover, the fitting values of charge transferred can be considered as a convex function of contact pressure which depends on the properties of Al and PTFE. This paper can not determine whether the correlation function of other tribo-pairs is convex but it is certain that the charge transferred and contact pressure are positively correlated<sup>7</sup>.

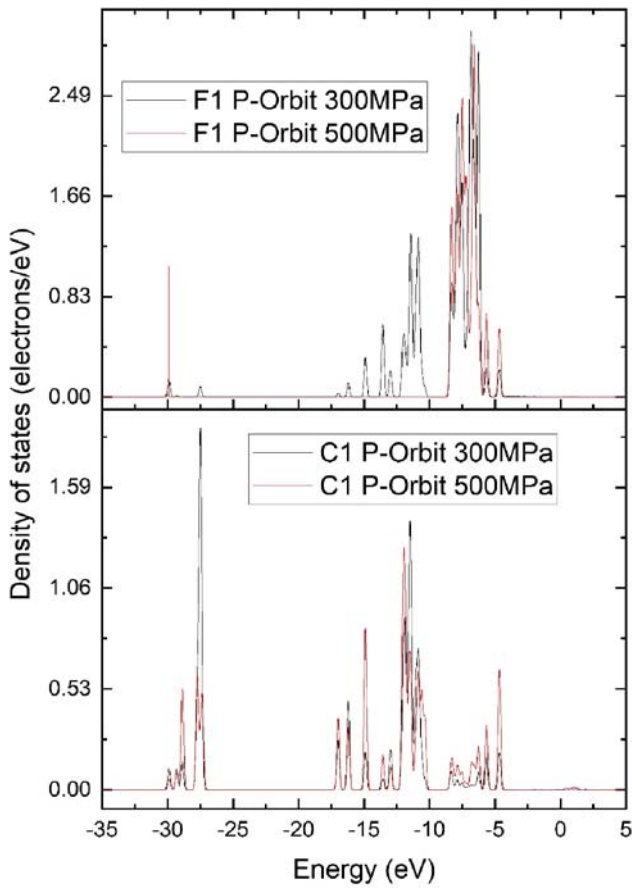


Figure 3. The projected DOS of the 2p orbital of F-atom 1 and C-atom 1

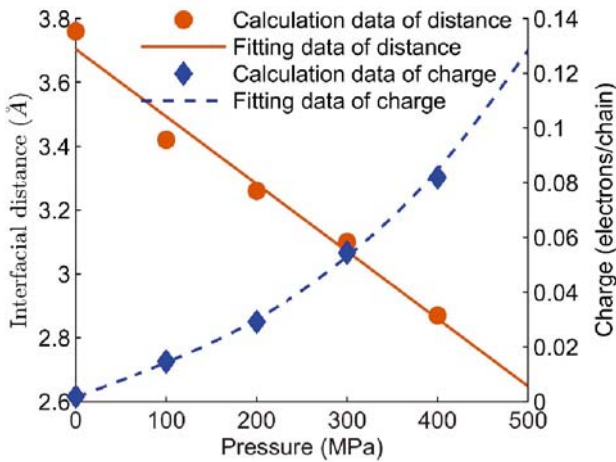


Figure 4. The relations between interfacial distance, charge transferred and contact pressure

**METHOD FOR FEM CALCULATIONS**

Section 2 introduces the CE mechanism of Al and PTFE tribo-layers which can be applied to sliding-mode TENG. The tribo-layers of sliding-mode TENG slide relatively under the action of friction. The fitting relation of contact pressure and charge transferred from Section 2 are the input variables of FEM calculations.

**Physical Field of Silding-Mode TENG**

Wang’s research team proposed the theory of sliding-mode TENG.(4) We adopt the same geometric parameters of their model and build a partial differential model in the Coefficient Form Interfaces of COMSOL. The

upper tribo-material is Al and the lower tribo-material is PTFE. And their thickness and width are 0.22 mm and 0.1 m respectively. The physical field of sliding-mode TENG is the electric field which can be described by Gauss’s law. To compare the energies among different contact pressures, the electric energy  $W_e$  is calculated via FEM method.

$$\nabla \cdot W_e = DE / 2 \tag{1}$$

Here,  $D$  is the electric displacement field,  $E$  is the electric field.

In many applications of sliding-mode TENG, the TENG aims to harvest the mechanical energy of some specific moving objects. It is worth noting but easy to ignore that there is friction loss in the system. Assuming the movement speed of the object is almost constant, the friction loss in one cycle  $W_f$  can be calculated by

$$W_f = fP\omega l^2 / 2 \tag{2}$$

Here,  $\omega$  is the width of sliding-mode TENG,  $l$  is the length of sliding-mode TENG,  $P$  is the contact pressure,  $f$  is the friction coefficient of friction surface between Al and PTFE and set to 0.1<sup>25</sup>. Finally, the recovered energy  $W_r$  can be deduced by

$$W_r = W_e - W_f \tag{3}$$

**Physical Field of FEM Simulation Results**

In this paper, the initial positions of two tribo-layers of sliding-mode TENG overlap. After a cycle of movement, the upper and lower tribo-layers will be just staggered. Figure 5 presents the electric potential of sliding-mode TENG when the tribo-layers move to the center position. Taking infinity as the reference point of zero potential, the maximum values of electric potential reach about  $1.6 \times 10^5$ ,  $5.9 \times 10^5$ ,  $1.4 \times 10^6$  V respectively, which correspond to the simulation results of 100, 300, 500 MPa. And the maximum electric field strengths are located where the tribo-layers are separated and about  $7.2 \times 10^8$ ,  $2.2 \times 10^9$ ,  $6.4 \times 10^9$  V/m respectively.

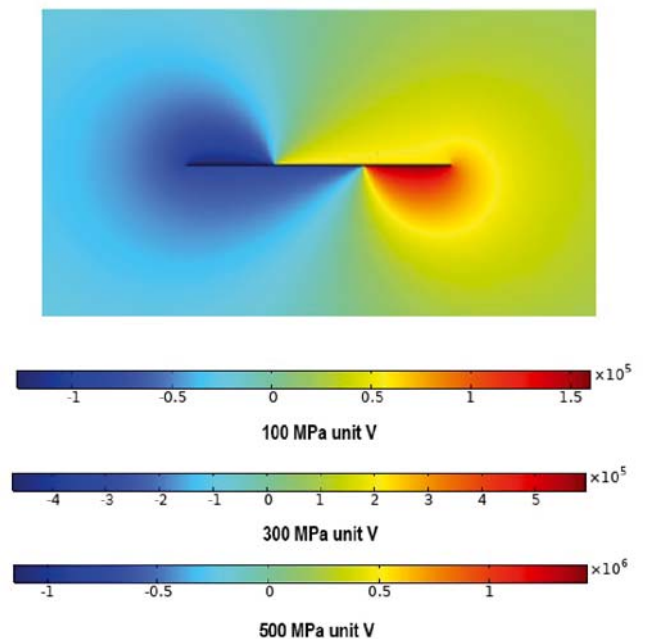
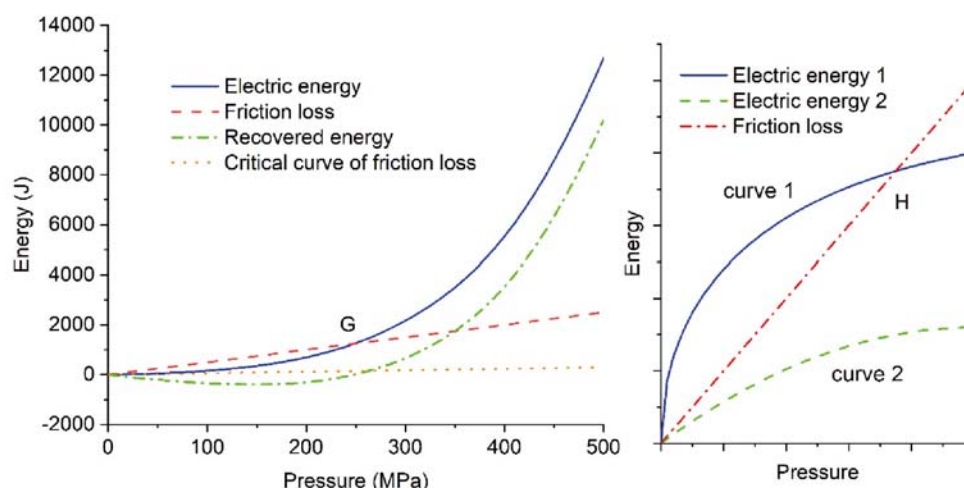


Figure 5. The electric potential of sliding-mode TENG



**Figure 6.** The relation between energies and contact pressure. (a) Al/PTFE tribo-pair model. (b) Tribo-pairs whose electric energy is a concave function of contact pressure

Figure 6 (a) is the relation between contact pressure and energies which are the electric energy, friction loss, recovered energy and critical curve of friction loss for Al/PTFE tribo-pair. The above energies are calculated by FEM software in one cycle. From Figure 6 (a), it can be seen that the friction loss with friction coefficient of 0.1 is proportional to the contact pressure which can also be seen in Equation 7. The electric energy is a convex function of contact pressure and this property depends on the relation of charge transferred and contact pressure which is shown in Figure 4. The recovered energy is negative until the contact pressure is larger than 248 MPa, which corresponds to point G. Moreover, the slope of the critical curve of friction loss is equal to 0.01178 which also equals the slope of the electric energy curve at zero pressure. For the tribo-pair Al/PTFE, such a small friction coefficient is difficult to achieve.

Considering the working limitations of TENG's actuators, there is a working pressure range. The optimum pressure is discussed in the following two cases:

(1) If the friction coefficient is greater than the critical value of 0.01178, the curve of electric energy and the curve of friction loss have two intersections which are the origin and the point G as shown in Figure 6 (a). According to the properties of the convex function, the recovered energy takes the maximum value at the lower or upper limit of the working pressure. Therefore, the boundary value of contact pressure corresponding to the larger recovered energy is the optimum pressure in the specific working pressure range. If the upper limit is up to 500 MPa, the recovered energy will be up to 10186.58 J per cycle.

(2) If the friction coefficient is smaller than the critical value, the difference between electric energy and friction loss increases with the increase of contact pressure. Therefore, the optimum pressure is equal to the upper limit of the working pressure. This strategy is covered in strategy (1).

The above strategies of optimum pressure are applied to the case where the electric energy is a convex function of contact pressure. The optimum pressure exists in most working conditions of sliding-mode TENG. If the working range of pressure is wide enough, the maximum contact pressure can provide the maximum recovered energy. Moreover, the recovered energy will

increase greatly if researchers can decrease the friction coefficient of tribo-layers which can be seen in Figure 6 (a). However, a reduction in the friction coefficient and an increase in the contact area of F and Al atoms may be contradictory which requires further research.

It can be envisaged that there exist such tribo-pairs whose electric energy and charge transferred are the concave functions of contact pressure. Figure 6 (b) shows the relations between electric energies and contact pressure for such tribo-pairs. There are curve 1 and 2 correspond to electric energy 1 and 2 and are discussed as follows:

(1) The slope of curve 1 at zero pressure is larger than the slope of the curve for friction loss. On curve 1, there exist two intersections with the curve for friction loss, which are the origin and point H. According to the properties of the concave function, there exists an arresting point which is between the origin and point H. The recovered energy of the arrest point is the maximum recovered energy when the pressure of the arrest point is within the working pressure range. In this case, the pressure of the arrest point is the optimum pressure. If the pressure of the arrest point is outside the working pressure range, the optimum pressure is equal to one of the two boundary pressure values, which corresponds to the larger recovered energy.

(2) The slope of curve 2 at zero pressure is smaller than the slope of the curve for friction loss. And the recovered energy of curve 2 is always negative and decreases with the increase of pressure. The optimum pressure is equal to the lower limit of working pressure. Therefore, the tribo-pairs corresponding to curve 2 are not suitable for harvesting energy.

## CONCLUSIONS

This research combines an ab initio calculation and a FEM simulation to study the mechanism of sliding-mode TENG. Via Quantum Espresso software package, the wavefunctions and electronic structures of Al/PTFE tribo-pair are calculated under the different contact pressure. It shows that the amount of charge transferred increases with the increasing overlap of the outer orbitals of F and Al atoms. Moreover, the interfacial distance decreases monotonically with contact pressure and the charge transferred can be fitted as a convex function of contact pressure.

The relation between contact pressure and the amount of charge transferred can be the lookup function of FEM simulation. Considering the friction loss and electric energy in one cycle, the recovered energy can be calculated. For the tribo-pairs whose electric energy is a convex function of pressure, the optimum pressure in the specific working pressure range is equal to the boundary value of working pressure corresponding to the larger recovered energy. To improve the recovered energy, we can increase the working pressure range, decrease the friction coefficient and increase the contact area of Al and F atoms.

## ACKNOWLEDGMENTS

This research was supported by Postgraduate Research & Practice Innovation Program of Jiangsu Province in 2020 (Project number: KYCX20\_3013).

## LITERATURE CITED

- Liu, D., Yin, X., Guo, H., Zhou, L., Li, X., Zhang, C., Wang, J. & Wang, Z.L. (2019). A Constant Current Triboelectric Nanogenerator Arising From Electrostatic Breakdown. *Sci. Adv.* 5, eaav6437. DOI: 10.1126/sciadv.aav6437.
- Zhou, Y., Shen, M., Cui, X., Shao, Y., Li, L. & Zhang, Y. (2021). Triboelectric Nanogenerator Based Self-Powered Sensor for Artificial Intelligence. *Nano Energy* 84, 105887. DOI: 10.1016/j.nanoen.2021.105887.
- Wang, Z.L. (2020). Triboelectric Nanogenerator (TENG)—Sparking an Energy and Sensor Revolution. *Adv. Energy Mater.* 10, pp. 2000137. DOI: 10.1002/aenm.202000137.
- Niu, S., Liu, Y., Wang, S., Lin, L., Zhou, Y.S., Hu, Y. & Wang, Z.L. (2013). Theory of Sliding-Mode Triboelectric Nanogenerators. *Adv. Mater.* 25, 6184–6193. DOI: 10.1002/adma.201302808.
- Wang, Z.L. (2020). On the First Principle Theory of Nanogenerators from Maxwell's Equations. *Nano Energy* 68, 104272. DOI: 10.1016/j.nanoen.2019.104272.
- Shen, X., Wang, A.E., Sankaran, R.M. & Lacks, D.J. (2016). First-Principles Calculation of Contact Electrification and Validation by Experiment. *J. Electrostat.* 82, 11–16. DOI: 10.1016/j.elstat.2016.04.006.
- Wu, J., Wang, X., Li, H., Wang, F. & Hu, Y. (2019). First-Principles Investigations on the Contact Electrification Mechanism between Metal and Amorphous Polymers for Triboelectric Nanogenerators. *Nano Energy* 63, 103864. DOI: 10.1016/j.nanoen.2019.103864.
- Tan, D., Willatzen, M. & Wang, Z.L. (2021). Electron Transfer in the Contact-Electrification between Corrugated 2D Materials: A First-Principles Study. *Nano Energy* 79, 105386. DOI: 10.1016/j.nanoen.2020.105386.
- Fatti, G., Righi, M.C., Dini, D. & Ciniero, A. (2020). Ab Initio Study of Polytetrafluoroethylene Defluorination for Tribocharging Applications. *ACS Appl. Polym. Mater.* 2, 5129–5134. DOI: 10.1021/acsapm.0c00911.
- Fu, R., Shen, X. & Lacks, D.J. (2017). First-Principles Study of the Charge Distributions in Water Confined between Dissimilar Surfaces and Implications in Regard to Contact Electrification. *J. Phys. Chem. C* 121, 12345–12349. DOI: 10.1021/acs.jpcc.7b04044.
- Song, J. & Zhao, G. (2019). A Theoretical Model to Predict Contact Electrification. *Tribol. Int.* 136, 234–239. DOI: 10.1115/1.4053580.
- Kulbago, B.J. & Chen, J. (2020). Nonlinear Potential Field in Contact Electrification. *J. Electrostat.* 108, 103511. DOI: 10.1016/j.elstat.2020.103511.
- Xu, C., Zhang, B., Wang, A.C., Cai, W., Zi, Y., Feng, P. & Wang, Z.L. (2019). Effects of Metal Work Function and Contact Potential Difference on Electron Thermionic Emission in Contact Electrification. *Adv. Funct. Mater.* 29, 1903142. DOI: 10.1002/adfm.201903142.
- Niu, S., Zhou, Y.S., Wang, S., Liu, Y., Lin, L., Bando, Y. & Wang, Z.L. (2014). Simulation Method for Optimizing the Performance of an Integrated Triboelectric Nanogenerator Energy Harvesting System. *Nano Energy* 8, 150–156. DOI: 10.1016/j.nanoen.2014.05.018.
- Niu, S., Liu, Y., Zhou, Y.S., Wang, S., Lin, L. & Wang, Z.L. (2015). Optimization of Triboelectric Nanogenerator Charging Systems for Efficient Energy Harvesting and Storage. *IEEE Trans. Electron Devices* 62, 641–647. DOI: 10.1109/TED.2014.2377728.
- Dai, K., Liu, D., Yin, Y., Wang, X., Wang, J., You, Z., Zhang, H. & Wang, Z.L. (2022). Transient Physical Modeling and Comprehensive Optimal Design of Air-breakdown Direct-Current Triboelectric Nanogenerators. *Nano Energy* 92, 106742. DOI: 10.1016/j.nanoen.2021.106742.
- Min, G., Manjakkal, L., Mulvihill, D.M. & Dahiya, R.S. (2020). Triboelectric Nanogenerator with Enhanced Performance via an Optimized Low Permittivity Substrate. *IEEE Sens. J.* 20, 6856–6862. DOI: 10.1109/JSEN.2019.2938605.
- Niu, S. & Wang, Z.L. (2015). Theoretical Systems of Triboelectric Nanogenerators. *Nano Energy* 14, 161–192. DOI: 10.1016/j.nanoen.2014.11.034.
- Jiang, T., Zhang, L.M., Chen, X., Han, C.B., Tang, W., Zhang, C., Xu, L. & Wang, Z.L. (2015). Structural Optimization of Triboelectric Nanogenerator for Harvesting Water Wave Energy. *ACS Nano* 9, 12562–12572. DOI: 10.1021/acsnano.5b06372.
- Scandolo, S., Giannozzi, P., Cavazzoni, C., de Gironcoli, S., Pasquarello, A. & Baroni, S. (2017). First-Principles Codes for Computational Crystallography in the Quantum-ESPRESSO Package. *J. Phys. Condens. Matter.* 29, 465901. DOI: 10.1524/zkri.220.5.574.65062.
- Fatti, G., Righi, M.C., Dini, D. & Ciniero, A. (2020). Ab Initio Study of Polytetrafluoroethylene Defluorination and Its Possible Effects on Tribocharging. *ACS Appl. Polym. Mater.* 2, 5129–5134. DOI: 10.1021/acsapm.0c00911.
- Clark, E.S. (1999). The molecular conformations of polytetrafluoroethylene: forms II and IV. *Polymer* 40, 4659–4665. DOI: 10.1016/S0032-3861(99)00109-3.
- D'Ilario, L. & Giglio, E. (1974). Calculation of the van der Waals Potential Energy for Polyethylene and Polytetrafluoroethylene as Two-Atom and Three-Atom Chains: Rotational Freedom in the Crystals. *Acta Cryst., B* 30, 372–378. DOI: 10.1107/S0567740874002846.
- Zhao, P., Soin, N., Prashanthi, K., Chen, J., Dong, S., Zhou, E., Zhu, Z., Narasimulu, A.A., Montemagno, C.D., Yu, L. & Luo, J. (2018). Emulsion Electrospinning of Polytetrafluoroethylene (PTFE) Nanofibrous Membranes for High-Performance Triboelectric Nanogenerators. *ACS Appl. Mater. Interfaces* 10, 5880–5891. DOI: 10.1021/acsami.7b18442.
- Babuska, T.F., Pitenis, A.A., Jones, M.R., Nation, B.L., Sawyer, W.G. & Argibay, N. (2016). Temperature-Dependent Friction and Wear Behavior of PTFE and MoS<sub>2</sub>. *Tribol. Lett.* 63, 1–7. DOI: 10.1007/s11249-016-0702-y.